



## OPEN Digestion in the arachnid *Mischonyx squalidus* as a probable source of lipids to synthesize opiliones defense and communication molecules

Jefferson Oliveira Silva<sup>1,2</sup>, Vincent Louis Viala<sup>1</sup>, Renata Oliveira Dias<sup>3</sup>, Clelia Ferreira<sup>4</sup>, Walter R. Terra<sup>4</sup>, Ricardo Pinto-da-Rocha<sup>5</sup> & Adriana Rios Lopes<sup>1,2</sup>✉

Opiliones (Arachnida) comprises approximately 7,000 species. Due to their lack of venom glands, their defense is mainly based on the secretion of scent glands, which also play roles in communication and antimicrobial activity. This odoriferous secretion has a diverse composition according to harvestmen species but frequently contains benzoquinones. Studies of benzoquinone synthesis intermediates suggest a pathway based on lipid metabolism from diet. This study provides the first transcriptomic and enzymatic analysis of the midgut of *Mischonyx squalidus* to understand the acquisition of nutrients. The enzymatic analysis tested 11 digestive enzymes and found high lipase activity and moderate and low activity for peptidases and carbohydrases, respectively. Transcriptome sequencing yielded 19,658 unigenes, predominating enzymes and binding proteins closely associated with Xiphosura and Scorpiones proteins; a third of which are hydrolases. A multigene lipase family is expressed. Cathepsin L peptidases were prominently abundant, indicating their relevance for protein digestion. Additionally, toxin-like proteins and lipid metabolism-related enzymes, such as phospholipase A<sub>2</sub> and NPC cholesterol transporters, were represented, indicating a sophisticated digestive and metabolic system for lipids. These findings suggest a link between lipid digestive metabolism and defensive and communicative molecule synthesis, underscoring Opiliones' unique evolutionary adaptations.

**Keywords** Opiliones, Digestion, Transcriptome, Enzymes, Lipids, *Mischonyx squalidus*

Opiliones is one of the largest orders in Arachnida, containing approximately 7,000 species distributed worldwide<sup>1</sup>. The group is omnivorous, with a preference for animal matter, and is the only group of arachnids that does not perform extra-oral digestion but bites off small pieces to ingest solid tissues<sup>2</sup>. Due to their lack of venom glands, Opiliones have not been mainly explored as a source of new enzymes and toxins even though the scent secretion produced by this Arachnida group has been the focus of studies regarding the production of benzoquinones and other organic compounds as antibiotics, such as gonyleptidine, a 2,5-dimethyl-1,4-benzoquinone identified in *Acanthopachylus aculeatus*<sup>2</sup>.

Biologically, the scent gland (SG) or repugnatorial glands are exocrine structures mainly involved in the Opiliones' defense from microorganisms and predators and communication with conspecifics. The chemistry of the scent gland has been detailed for about 2% Opiliones species since the discovery of Ernest Hofer of the European harvestmen *Phalangium opilio* quinones<sup>3–7</sup>. The major chemical classes of secretion components are phenols, benzoquinones, ketones, and alkaloids<sup>8</sup>. The nature of some of those molecules indicates that their synthesis starts with molecules derived from lipid metabolism, such as acetate and propionate identified in

<sup>1</sup>Laboratory of Biochemistry, Instituto Butantan, São Paulo 05503900, Brazil. <sup>2</sup>Biotechnology Postgraduate Program, University of São Paulo, São Paulo 05508000, Brazil. <sup>3</sup>Laboratory of Genetics and Biodiversity, Goiás Federal University, Goiânia 74045155, Brazil. <sup>4</sup>Department of Biochemistry, Institute of Chemistry, University of São Paulo, São Paulo 05508900, Brazil. <sup>5</sup>Department of Zoology, Institute of Biosciences, University of São Paulo, São Paulo 05508090, Brazil. ✉email: adriana.lopes@butantan.gov.br

*Iporangaia pustulosa*<sup>9</sup> and *Mischnonyx squalidus*<sup>10</sup> which are produced via the malonyl-CoA pathway. These data suggest that fatty acids and/or acetyl-CoA from food catabolism would be essential to odour molecule synthesis.

Information regarding nutrient acquisition and digestive physiology are scarce in Opiliones, although the midgut is the largest organ in harvestmen. The foregut and hindgut, as usually in other arthropods, are cuticular lining tissues due to their ectodermic origins, while the midgut is a secretory epithelium due to its endodermic origin<sup>11</sup>. Similarly to other Arachnida species, the harvestmen midgut is divided into ventriculus and diverticula, and the monolayer digestive epithelium is composed mainly of secretory and digestive cells. However, harvestmen have a specific kind of cell, the resorptive cells, with vesicles containing material for the peritrophic membranes<sup>12</sup>. Although the morphology of the midgut is quite well known, the molecular physiology of harvestmen digestion is still unexplored.

Combined studies of enzymology and transcriptomic sequencing of Arachnida midgut samples have shed light on the molecular aspects of digestion in scorpions<sup>13</sup> spiders<sup>14,15</sup> ticks<sup>16</sup> and mites<sup>17</sup> allowing comparative and evolutive studies among predators with preoral digestion and hematophagous Arachnida, but data on saprophytic arachnids are missing. *M. squalidus* (former *M. cuspidatus*<sup>18</sup> is an omnivorous animal with saprophytic habits<sup>19</sup>. Several aspects of the biology of *M. squalidus* have been extensively studied, including the chemical composition of the scent glands' secretion, defensive behavior<sup>20–22</sup> odour sensitivity<sup>23</sup> and synanthropic behavior<sup>24</sup>.

In order to amplify the knowledge on Opiliones digestion and understand the possible communication between the digestive system as a source of lipids to the synthesis of odour molecules in this work, we have performed the first transcriptomic and carbohydrases, peptidases, and lipase activity analysis of the midgut of harvestmen, using *M. squalidus* as our studied model to understand the molecular aspects of digestion in Opiliones.

## Results

### Specific activities of digestive enzymes

Enzyme activities of lipases ( $561 \pm 71$  mU/mg), chitinase ( $0.2 \pm 0.05$  mU/mg), hexosaminidase ( $0.2 \pm 0.08$  mU/mg), alpha-L-fucosidase ( $0.41 \pm 0.07$  mU/mg), alpha-D-mannosidase ( $0.37 \pm 0.1$  mU/mg), cysteine peptidase (cathepsin L) ( $2.44 \pm 1.4$  mU/mg), aminopeptidase ( $6.77 \pm 4.5$  mU/mg) and carboxypeptidase ( $0.35 \pm 0.08$  mU/mg) were quantified in the midgut samples of *M. squalidus* (Table 1 and Fig. 1). Serino-peptidases (trypsin), metallopeptidases and  $\alpha$ -amylase activities were undetectable.

### Transcriptome assembly and gene ontology

The transcriptome of *M. squalidus* was assembled using trimmed reads from midgut samples, totalling 15,146,657 paired-end reads. *De novo* assembly resulted in 71,463 contigs. The translation of transcripts, considering only sequences with a predicted domain, yielded 25,462 protein sequences. The final transcript set, obtained after isoform removal, comprised 19,658 unigenes with BUSCO completeness scores of 64.5% for the Arachnida dataset and 77.3% for the Eukaryota dataset. The depth of the libraries for this assembly was between 13.8 and 26.7 (Supplementary Table 1).

Protein sequence annotation with Blastp analysis against the Invertebrate NCBI database resulted in a total of 16,957 sequences (86%) with Blast hits. The remaining 14% of sequences that did not show any identity with other annotated proteins at this stage were not investigated further. Most of the hits had as best hits sequences from *Limulus polyphemus* (2,945 sequences), followed by *Centruroides vittatus* (2,005 sequences), and *Centruroides sculpturatus* (1,390 sequences). Gene Ontology (GO) mapping has revealed that the predominant biological processes involve metabolic processes (2392 genes) and cellular processes (3186 genes), biological regulation (993 genes), and cellular component organisation or biogenesis (913 genes). The predominant molecular functions are catalytic activity (2368 genes) and binding (3535 genes) (Fig. 2).

Enzyme	Specific Activity (mU/mg)
Lipase	561 ± 71
Chitinase	0.2 ± 0.05
Hexosaminidase	0.20 ± 0.08
$\alpha$ -L-Fucosidase	0.41 ± 0.07
$\alpha$ -Mannosidase	0.37 ± 0.10
Aminopeptidase	6.77 ± 4.5
Cathepsin L	2.44 ± 1.4
Carboxypeptidase	0.35 ± 0.08
Serine peptidase	*
Astacin	*
$\alpha$ -Amylase	*

**Table 1.** Specific activities (mU/mg) of soluble digestive enzymes at *Mischnonyx squalidus* midguts ( $N=8$ ). The values are represented as mean followed by the standard deviation of specific digestive enzyme activities. The assay conditions are detailed in Table 6. The enzymes with an asterisk in the “specific activity” column had no activity detected.

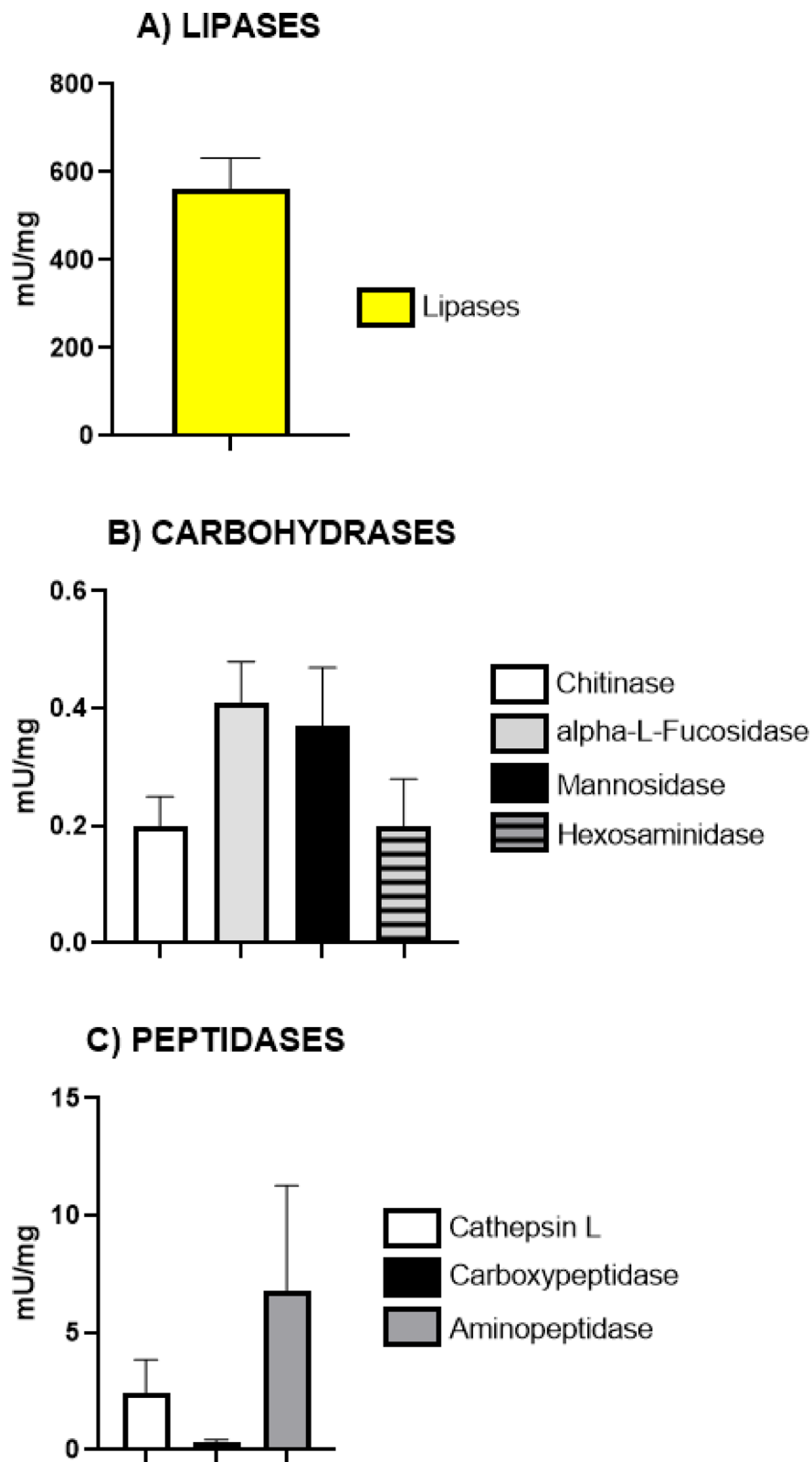


**Fig. 1.** Specific activities (mU/mg) of digestive enzymes measured at the soluble fraction of midgut samples from *M. squalidus*. Enzyme assays were performed, as shown in Table 6.  $N=8$  to each enzyme, except for carboxypeptidase (1 C)  $N=7$ . The error bars are SEM.

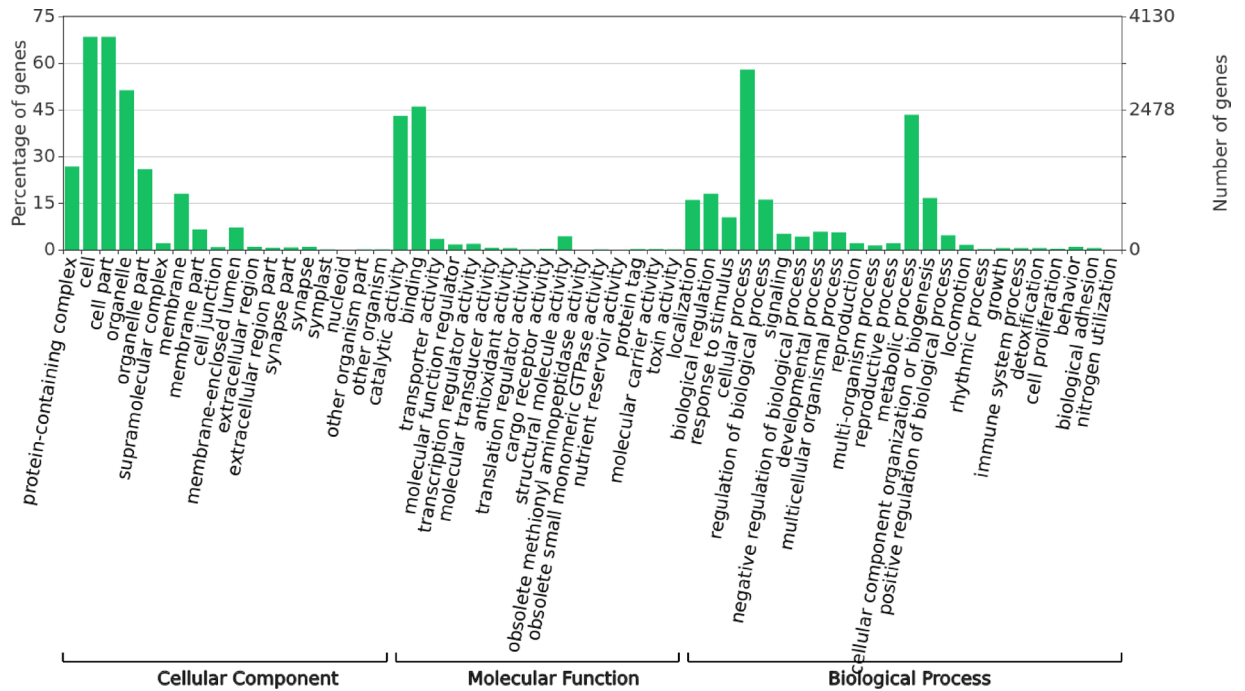


**Fig. 2.** Gene Ontology (GO) functional categorisation of the unigenes from *M. squalidus* midgut.

The top thirty unigenes with higher TPM values (ranging from 2,159.51 to 11,326.92) from *M. squalidus* midgut are mainly housekeeping genes and metabolic demands proteins (Supplementary Table 2). The only genes directly related to digestion are two peptidases annotated as putative cathepsins L (the top two most expressed transcripts in Table 2), indicating some relevance to digestive enzymes. Other highly expressed genes are from oxidative stress response elements (e.g., Glutathione S-Transferase; soma ferritin-like), which might be indirectly associated with food intake.

Functional annotation and classification based on EC numbers of the enzymes revealed a set of 2434 sequences annotated across the seven EC classes (Fig. 3A), with the majority corresponding to hydrolases and transferases. Focusing on hydrolases (EC 3.-), which mainly represent the enzymes involved in digestion, the classification by subclass revealed significant functional diversity. Among the 824 hydrolase sequences, 334 were classified as acting on acid anhydrides (EC 3.6.-), while 159 as acting on peptide bonds (peptidases) (EC 3.4.-), 152 as acting on ester bonds (EC 3.1.-), 123 as general hydrolases (EC 3.-), 39 as glycosylases (EC 3.2.-) and 27 as acting on carbon-nitrogen bonds, other than peptide bonds (EC 3.5.-). Other hydrolases EC were annotated for 10 unigenes (Fig. 3B).

The most abundant genes in the midgut (TPM > 50) that are effectively associated with digestion (Table 2) provide a clear view of this arachnid's digestive adaptations. The cysteine peptidase group comprises five annotated genes for cathepsin L, two of which have TPM values higher than 4000; one for cathepsin B, one for cathepsin O, and one for legumain. Among the other endopeptidases are nine serine endopeptidases: three trypsin-like isoforms (sum of TPM = 3540), two chymotrypsin-like (sum of TPM = 161,77), and two prolyl endopeptidases (sum of TPM = 185,73). Four metallopeptidases from the astacin family were identified (sum of TPM = 362). Exopeptidases totalize 20 distinct contigs with a sum of TPM of 4042, being the three most abundant expressed transcripts annotated as dipeptidyl-peptidase, carboxypeptidase B and aminopeptidase (Table 3).

Enzymes hydrolysing ester bonds, which include lipases and phospholipases, are the third hydrolase class with a higher number of transcripts assembled at the midgut transcriptome of *M. squalidus* (Fig. 3). When comparing the expression values, the pancreatic triacylglycerol lipases are the most highly expressed genes (with four transcripts totalling 586.1 TPMs) among this class, although gastric triacylglycerol lipases and monoglyceride lipases are also present (Table 4), as well as other 13 related transcripts. Blastp analysis of lipase evidenced best hits with spider lipases. Lipase sequence molecular modelling (Fig. 4) of human lipase opened conformation, closed horse lipase (Fig. 4A), *M. squalidus* lipase (Fig. 4B), insect lipase (Fig. 4C) and, spider lipase (Fig. 4D) evidenced the conservation of the catalytic triad (Ser, His Asp), the absence of a lid at *M. squalidus* and insect lipase structure suggesting an opened conformation<sup>25</sup> the presence and distinct structure organisation at the surroundings of the active site at spider lipase (Fig. 4D).

Besides the classic lipases involved in digestion, two phospholipases, patatin-like and phospholipase A2, were also identified with TPM values ranging from 50 to 120. Alpha-L-fucosidase-like (TPM = 1120), is the most expressed glycosidase transcript, followed by sucrase-isomaltase (TPM = 376.48) and alpha-mannosidase (TPM = 374.90), which were moderately expressed. Two chitinase-3-like (TPM = 271.87 and 238.92) and a beta-hexosaminidase (TPM = 207) indicate a moderate expression for the chitin-degrading enzymes complex. A unigene annotated for pancreatic alpha-amylase (TPM = 93.68) was also found (Table 5).

Sequence ID	Description	Length (bp)	TPM	Hit ACC
TRINITY_DN214_c0_g1_i1	Procathepsin L-like	334	4698.18	XP_055946881
TRINITY_DN1533_c0_g1_i1	Cathepsin L	335	4047.01	XP_029838979
TRINITY_DN373_c0_g2_i2	Legumain-like	458	1768.71	XP_054710296
TRINITY_DN309_c0_g1_i1	Trypsin-1-like	282	1698.93	XP_037290901
TRINITY_DN4472_c0_g1_i1	Cathepsin B-like	336	1335.42	XP_042911942
TRINITY_DN42886_c0_g1_i1	LOW QUALITY PROTEIN: trypsin-1-like	282	1111.50	XP_037277741
TRINITY_DN108_c0_g1_i11	Procathepsin L-like	334	847.87	XP_055940771
TRINITY_DN31_c0_g1_i10	Trypsin-1-like	302	729.59	XP_067140795
TRINITY_DN115_c0_g1_i1	Cathepsin L	331	406.55	XP_029838979
TRINITY_DN115_c0_g2_i1	Cathepsin L	354	269.50	XP_029838979
TRINITY_DN43986_c0_g1_i1	Astacin-like metalloprotease toxin 5	242	142.41	XP_055936909
TRINITY_DN989_c1_g2_i1	Prolyl endopeptidase FAP-like	765	125.44	XP_022237849
TRINITY_DN756_c0_g1_i2	Cathepsin L-like	453	125.23	XP_054714238
TRINITY_DN1895_c0_g1_i2	Cathepsin O-like	332	97.37	XP_023229439
TRINITY_DN1143_c0_g1_i1	Chymotrypsinogen A-like isoform X1	266	97.34	XP_022249622
TRINITY_DN23322_c0_g1_i1	Cathepsin L1-like isoform X2	334	95.32	XP_022236235
TRINITY_DN36302_c0_g1_i1	Serine protease filzig	138	86.43	XP_042898784
TRINITY_DN2723_c0_g1_i2	Zinc metalloproteinase nas-4-like	250	80.85	XP_013778641
TRINITY_DN1563_c0_g3_i1	Matrix metalloproteinase-19-like isoform X4	262	80.52	XP_046913389
TRINITY_DN1330_c0_g1_i2	Chymotrypsinogen A-like isoform X1	443	64.43	XP_022249622
TRINITY_DN15364_c0_g1_i1	Cathepsin L-like	141	64.14	XP_013794403
TRINITY_DN7206_c0_g2_i2	Prolyl endopeptidase-like	786	60.29	XP_023217988
TRINITY_DN8682_c0_g1_i2	Astacin-like metalloprotease toxin 1	281	58.75	XP_022241326
TRINITY_DN33712_c0_g1_i1	Serine proteinase stubble-like	280	50.10	XP_013787774

**Table 2.** Expression profile of the transcripts annotated as coding for putative endopeptidases in the midgut transcriptome of *Mischonyx squalidus*, ranked by the mean TPM of three samples.

### Analysis of digestive physiology-related and toxin-like proteins

Besides transcripts coding for digestive enzymes, some other essential transcripts were highly expressed in the midgut from *M. squalidus* (Supplementary Table 3). The most variable and expressed ones are peptidase inhibitors such as four-domain peptidase inhibitors (six unigenes, TPM sum=3,061) and intracellular coagulation inhibitor 1 & 2 (three unigenes, TPM sum=869). Another protein related to the digestive process in Arthropoda is peritrophin-like, identified by its domain CBM\_14, with its highest unigene presenting TPM value of 2,071 at *M. squalidus* midgut transcriptome.

Although harvestmen do not present a venom gland nor venomous secretions, some toxin-like proteins, typical of other arthropods' venoms, are present as transcripts at the midgut of this harvestmen species, such as U-24 ctenitoxin (average identity of 45%, e-value  $6 \times 10^{-37}$ ), scoloptoxin (identity=48,97%, e-value=0), and dermo necrotic toxin (identity=45,79%, e-value= $2 \times 10^{-96}$ ) and phospholipase A2 (identity=42,92%, e-value= $4 \times 10^{-64}$ ), usually associated to Hymenoptera venoms<sup>26</sup>.

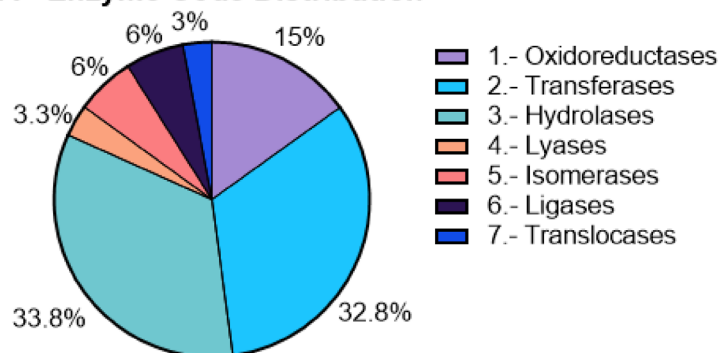
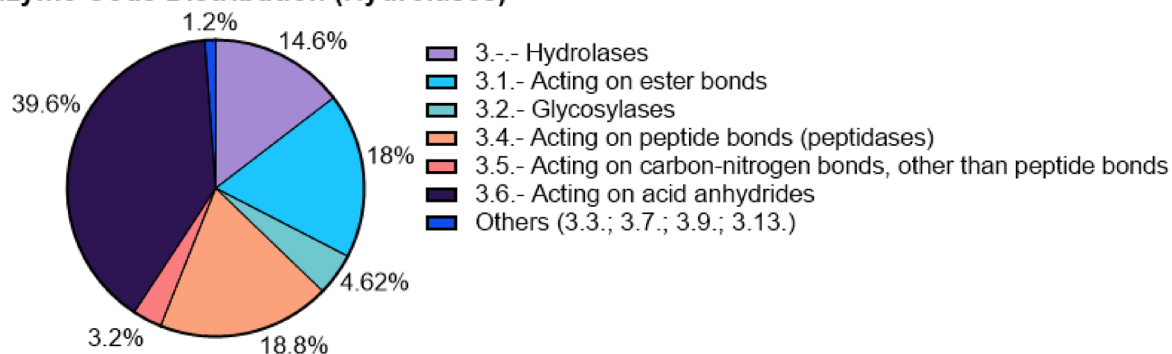
Transferases and translocases are groups of enzymes that are also highly expressed in *M. squalidus* midgut. Among transferases, glutathione S-transferases had 35 isoforms (TPM > 50) and high TPM values (Supplementary Table 3). Among translocases, V-type proton ATPase and sodium/potassium transporting ATPase were the most common and expressed genes.

NPC intracellular cholesterol transporters, which are likely involved in lipid metabolism, particularly in the intracellular transport and regulation of cholesterol export from lysosomes<sup>27</sup> were also highly represented (Supplementary Table 3).

## Discussion

### Digestive physiology in *M. squalidus* based on biochemical and transcriptomic analysis

In this work, the midgut of a harvestmen species was molecularly characterised for the first time through enzyme assays and RNA sequencing analyses. The enzymological analysis revealed high lipase activity, mainly acidic endopeptidase activities and a high activity of some exopeptidase, and lysosomal-like carbohydrases as the most active enzymes. The biochemical data agree with the transcriptomic data. The prevalence of hydrolases acting on acid anhydrides (EC 3.6.-) among the hydrolases (Fig. 3B) suggests that the majority of hydrolase genes in the midgut are essential for processes of translation (e.g. *Elongation Factor 1-alpha*) and stress response (e.g. *heat shock protein HSP 90-alpha-like*) suggesting high protein synthesis in this tissue (Supplementary Table 2). The subsequent high percentage of hydrolases functioning as peptidases, glycosylases, and hydrolases acting on ester bonds indicates enzymes that play a role in digestion and nutrient acquisition, breaking down peptides, carbohydrates, and lipids, respectively.

**A - Enzyme Code Distribution****B - Enzyme Code Distribution (Hydrolases)**

**Fig. 3.** Enzyme classes at the midgut of *M. squalidus*. (3A) Enzyme code distribution in the main class and (3B) hydrolases code distribution for *M. squalidus* midgut transcriptome assembly.

Sequence ID	Description	Length (bp)	TPM	Hit ACC
TRINITY_DN212_c0_g1_i1	Dipeptidyl peptidase 1-like	450	837.05	XP_054717755
TRINITY_DN1742_c0_g1_i1	Carboxypeptidase B-like	428	627.52	XP_022254702
TRINITY_DN579_c0_g1_i1	Putative aminopeptidase W07G4.4 isoform X2	571	351.11	XP_037528160
TRINITY_DN1027_c0_g1_i1	Probable serine carboxypeptidase CPVL	499	327.61	XP_013774685
TRINITY_DN2029_c0_g1_i1	Retinoid-inducible serine carboxypeptidase-like	443	260.24	XP_067143361
TRINITY_DN48358_c0_g1_i1	Lysosomal Pro-X carboxypeptidase	244	210.62	XP_067139333
TRINITY_DN504_c0_g1_i1	Carboxypeptidase Q-like, partial	288	201.18	XP_054158512
TRINITY_DN845_c0_g1_i1	Carboxypeptidase N subunit 2-like	465	150.10	XP_054162905
TRINITY_DN654_c0_g1_i4	Carboxypeptidase N subunit 2-like	364	143.60	XP_063532610
TRINITY_DN711_c0_g1_i20	Carboxypeptidase N subunit 2-like	313	139.33	XP_054718796
TRINITY_DN1145_c0_g1_i1	Dipeptidyl peptidase 3-like	763	135.80	XP_013773196
TRINITY_DN1932_c0_g1_i1	Carboxypeptidase N subunit 2-like	450	109.06	XP_054162905
TRINITY_DN943_c0_g1_i2	Cytosol aminopeptidase-like	531	96.74	XP_013778400
TRINITY_DN26138_c0_g1_i1	Carboxypeptidase B-like	109	70.68	XP_035228738
TRINITY_DN39723_c0_g1_i1	Puromycin-sensitive aminopeptidase	147	67.08	XP_030829988
TRINITY_DN1856_c0_g1_i1	Probable aminopeptidase NPEPL1	520	66.99	XP_022247313
TRINITY_DN22882_c0_g1_i1	Lysosomal Pro-X carboxypeptidase-like	216	65.73	XP_022253531
TRINITY_DN3369_c0_g1_i8	Tripeptidyl-peptidase 2	835	65.46	XP_067127626
TRINITY_DN48182_c0_g1_i1	Methionine aminopeptidase 1-like	376	65.43	XP_013774336
TRINITY_DN8849_c0_g1_i2	Carboxypeptidase N subunit 2-like	193	51.13	XP_054718796

**Table 3.** Expression profile of the transcripts annotated as coding for putative exopeptidases in the midgut transcriptome of *Mischonyx squalidus*, ranked by the mean TPM of three samples.

Sequence ID	Description	Length (bp)	TPM	Hit ACC
TRINITY_DN5309_c0_g1_i1	Pancreatic triacylglycerol lipase-like isoform X1	554	264.44	XP_055945860
TRINITY_DN2466_c0_g1_i1	Pancreatic triacylglycerol lipase-like isoform X1	498	198.95	XP_022258928
TRINITY_DN466_c0_g1_i1	Pancreatic lipase-related protein 2-like isoform X1	380	176.24	XP_013782252
TRINITY_DN950_c0_g1_i1	Gastric triacylglycerol lipase-like	338	153.94	XP_023224000
TRINITY_DN1811_c0_g1_i1	Pancreatic lipase-related protein 2-like	269	137.07	XP_067140005
TRINITY_DN718_c0_g1_i1	Phospholipase A2-like isoform X1	337	120.09	XP_055935287
TRINITY_DN33629_c0_g1_i1	Monoglyceride lipase-like	285	111.82	XP_067128874
TRINITY_DN93_c0_g1_i1	PREDICTED: isoamyl acetate-hydrolyzing esterase 1 homolog	265	110.64	XP_002734595
TRINITY_DN1131_c0_g1_i2	Pancreatic lipase-related protein 2-like isoform X2	517	82.20	XP_022250239
TRINITY_DN7209_c0_g1_i1	Acidic phospholipase A2 Cc1-PLA2	158	76.69	XP_014780833
TRINITY_DN8441_c0_g2_i1	Pancreatic triacylglycerol lipase-like	400	68.34	XP_022244501
TRINITY_DN38441_c0_g1_i1	Monoglyceride lipase-like	208	65.61	XP_067128874
TRINITY_DN677_c0_g1_i4	Gastric triacylglycerol lipase-like	420	64.62	XP_023224000
TRINITY_DN4295_c0_g1_i1	Monoacylglycerol lipase ABHD12-like isoform X4	330	60.24	XP_023210082
TRINITY_DN5044_c0_g1_i1	Pancreatic lipase-related protein 2-like isoform X2	505	59.68	XP_022250239
TRINITY_DN52228_c0_g1_i1	Group 3 secretory phospholipase A2-like	278	55.81	XP_035213327
TRINITY_DN3371_c0_g1_i1	Patatin-like phospholipase domain-containing protein 2	732	55.23	XP_022239037
TRINITY_DN1588_c0_g2_i1	Pancreatic triacylglycerol lipase-like isoform X2	287	54.37	XP_035216469
TRINITY_DN2895_c0_g1_i1	Putative phospholipase B-like 2	251	50.98	XP_054714812

**Table 4.** Expression profile of the transcripts annotated as coding for putative lipases in the midgut transcriptome of *Mischonyx squalidus*, ranked by the mean TPM of three samples.

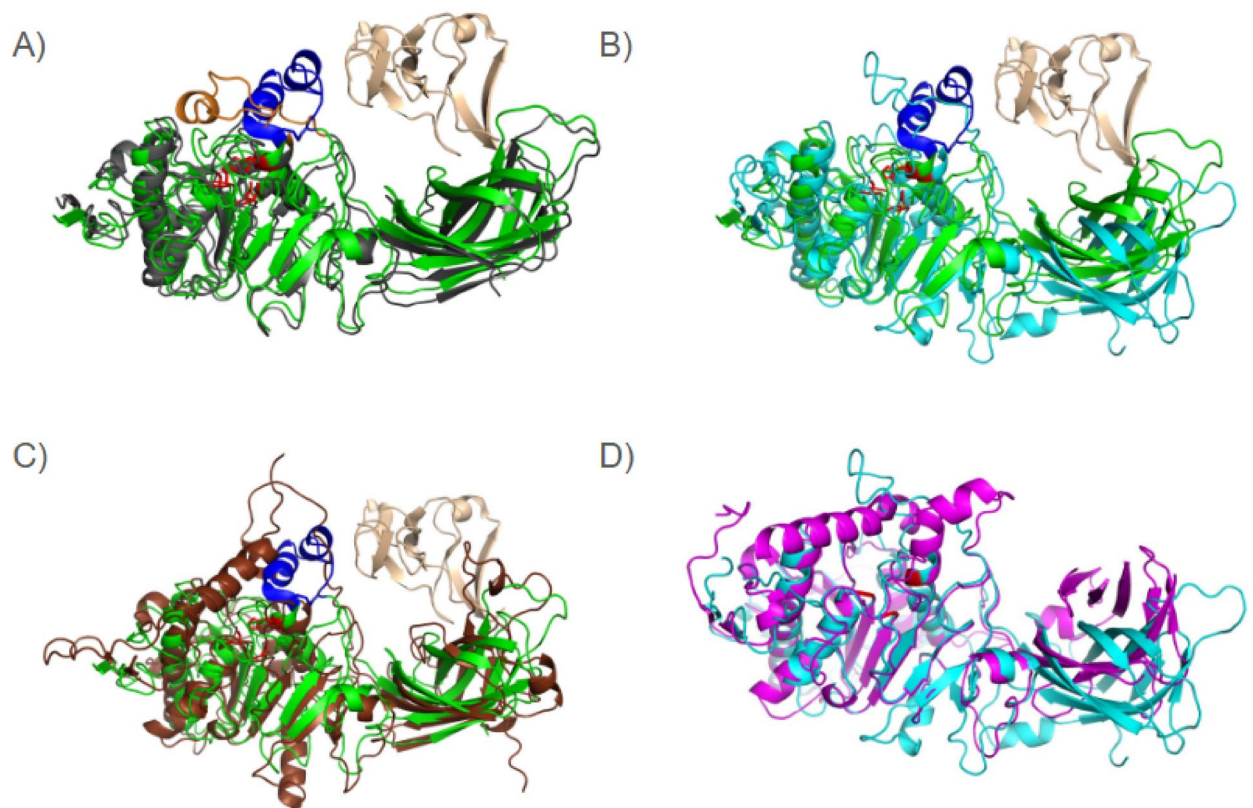


**Fig. 4.** Molecular modelling of distinct lipases. The catalytic residues are in red in all lipase structures. (A) Human pancreatic lipase in open conformation (PDB 1LPA, in green) and horse pancreatic lipase in close conformation (PDB 1HPL, in grey). In dark blue, the lid of LPA and in orange the lid of HPL, in wheat the colipase structure bound to LPA. (B) LPA and *M. squalidus* lipase DN4626\_c0\_g1\_i1.p1 (this work in cyan), (C) LPA and *Spodoptera frugiperda* (GenBank accession number XP\_050561712.1PTL in brown) and, (D) *M. squalidus* lipase in cyan and spider *Nephilingis cruentata* lipase (SRR3943479) in magenta.

Sequence ID	Description	Length (bp)	TPM	Hit ACC
TRINITY_DN6263_c0_g1_i3	Alpha-L-fucosidase-like isoform X1	474	1120.54	XP_054707937
TRINITY_DN150_c0_g1_i1	Sucrase-isomaltase, intestinal-like	785	376.48	XP_022245029
TRINITY_DN698_c0_g1_i1	Lysosomal alpha-mannosidase-like isoform X1	865	374.90	XP_055941111
TRINITY_DN2379_c0_g1_i1	Chitinase-3-like protein 1	580	271.87	XP_022240293
TRINITY_DN1845_c0_g1_i2	Chitinase-3-like protein 1	491	238.92	XP_067124007
TRINITY_DN3076_c0_g1_i1	Beta-glucuronidase	646	214.38	XP_067130244
TRINITY_DN641_c0_g1_i15	Beta-hexosaminidase subunit alpha-like isoform X1	534	207.25	XP_035223338
TRINITY_DN11221_c0_g3_i2	Probable chitinase 10	504	165.89	XP_023225350
TRINITY_DN2923_c0_g1_i1	Glucosidase 2 subunit beta-like	548	159.65	XP_055926585
TRINITY_DN899_c0_g1_i12	Beta-galactosidase-like	539	157.40	XP_067119019
TRINITY_DN961_c0_g1_i1	Alpha-L-fucosidase-like isoform X2	104	153.77	XP_064478245
TRINITY_DN742_c0_g1_i1	Beta-hexosaminidase subunit alpha-like	571	113.13	XP_013774138
TRINITY_DN1718_c0_g1_i1	Maltase 1-like	566	108.47	XP_022254812
TRINITY_DN2739_c0_g1_i1	Maltase 1-like	105	98.01	XP_022254812
TRINITY_DN7097_c0_g1_i1	Neutral alpha-glucosidase AB-like	925	96.19	XP_023222247
TRINITY_DN2811_c0_g1_i4	Maltase-glucoamylase, intestinal-like	955	94.98	XP_035212239
TRINITY_DN2521_c0_g1_i1	Pancreatic alpha-amylase	525	93.68	XP_021002580
TRINITY_DN613_c0_g1_i1	Beta-galactosidase-like	645	90.93	XP_067119019
TRINITY_DN1083_c0_g1_i1	Glucosylceramidase-like isoform X1	528	86.13	XP_013790006
TRINITY_DN1248_c0_g1_i4	LOW QUALITY PROTEIN: maltase-glucoamylase, intestinal-like	900	85.34	XP_022251203
TRINITY_DN1315_c0_g1_i1	LOW QUALITY PROTEIN: maltase-glucoamylase, intestinal-like	221	82.01	XP_022251203
TRINITY_DN1176_c0_g1_i2	Beta-galactosidase-like isoform X1	560	72.36	XP_013783507
TRINITY_DN3179_c0_g1_i14	Lysosomal alpha-glucosidase-like	309	66.07	XP_022249729
TRINITY_DN40176_c0_g1_i1	Probable chitinase 10	244	65.04	XP_057371454
TRINITY_DN3823_c0_g1_i2	ER degradation-enhancing alpha-mannosidase-like protein 1	588	60.51	XP_067124664
TRINITY_DN1381_c0_g1_i3	LOW QUALITY PROTEIN: maltase-glucoamylase, intestinal-like	933	58.76	XP_022251203
TRINITY_DN2896_c0_g1_i1	Hexosaminidase D-like	658	55.59	XP_055937155
TRINITY_DN3255_c0_g1_i1	Sucrase-isomaltase, intestinal-like isoform X2	147	53.92	XP_064456553
TRINITY_DN8416_c0_g1_i1	Chitotriosidase-1-like isoform X2	339	53.33	XP_052262852
TRINITY_DN1781_c0_g1_i3	Mannosyl-oligosaccharide glucosidase-like	595	51.53	XP_022241665

**Table 5.** Expression profile of the transcripts annotated as coding for putative carbohydrases in the midgut transcriptome of *Mischonyx squalidus*, ranked by the mean TPM of three samples.

Sequence annotation of enzymes involved in carbohydrate processing highlights the presence of transcripts for chitinase, fucosidase, mannosidase, and hexosaminidase, which were usually identified as digestive enzymes in previous Arachnida digestion analyses<sup>13–15</sup>. Among these carbohydrases, an alpha-L-fucosidase (Table 5) is the most abundant carbohydrase transcript in the digestive tissue, followed by an alpha-mannosidase-like transcript. Experiments of cell fractionation and proteomic analysis of the midgut diverticula from the spider *Nephilingis cruentata* evidenced that fucosidase, mannosidase and a series of carbohydrases involved in monomers removing are lysosomal enzymes involved in the intracellular phase of digestion. Similar results were obtained in the proteomic analysis of the digestive fluid and abdomen from *Acanthoscurria geniculata*<sup>28</sup> suggesting that fucosidase and mannosidase are lysosomal enzymes. *M. squalidus* is the first Arachnida species that has higher expression and activity of typical lysosome-like carbohydrases as the main enzymes processing carbohydrates instead of chitinases. Thus, comparing data obtained from *M. squalidus* with those from spiders' digestive enzymes suggests that Opiliones have a more relevant carbohydrate degradation during intracellular digestion than extracellular digestion. Only a single transcript with a very low TPM value was identified in the transcriptome as *pancreatic alpha-amylase*, which is coherent with the absence of activities at the enzymatic assays. This enzyme's low expression and activity might suggest that starch/glycogen digestion is not a metabolic priority for *M. squalidus*, likely due to its saprophytic feeding habit or specific ecological niche. However, these animals had sucrase-isomaltase (TPM=376.48) and maltase-glucoamylase (TPM=94.98), which might catalyse the hydrolysis of glucose oligomers shorter than starch or glycogen. This hypothesis is coherent with the harvestmen saprophytic feeding habit. Complex carbohydrates like starch might have already been partially digested and ingested as oligosaccharides, suggesting adaptations for digesting partially degraded carbohydrates. However, this distribution of carbohydrases is distinct from the pattern presented by spiders, scorpions, and even mites and ticks, where transcripts coding depolymerases such as chitinases and amylases are the most abundant transcripts and amylase and chitinase activities are higher in comparison to lysosomal-like carbohydrases, such as fucosidase and mannosidase<sup>14</sup>.

Distinctly from carbohydrases, peptidase activities from *M. squalidus* are similar to those peptidases identified in ticks, scorpions and spiders midgut: acidic peptidases, mainly cathepsin L-like cysteine peptidases

of multiple isoforms. *M. squalidus* has 10 annotated cathepsin L unigenes, four of which are highly expressed with a TPM of 4,698.18 coding pro cathepsin L-like. Other RNA sequence coding cysteine peptidases and also highly expressed codes legumain and cathepsins B and O. Although the level of expression of cathepsin L is similar to other Arachnida species, the activity measured to *M. squalidus* is significantly lower compared to species, such as *Uloborus sp.*<sup>15</sup> and *T. serrulatus*<sup>13</sup> (Fig. 5). Some possible hypotheses for that are an insufficient cathepsin L zymogen activation; high degree of autolysis or inhibition by an excess of substrate in a complex midgut homogenate sample. Another possibility is the inhibition by the cathepsin propeptide inhibitor domain (I29), also identified at the *M. squalidus* cathepsin L sequences in the transcriptome, which can be a competitive inhibitor with the substrate even after enzyme activation (Table 1).

Regardless of this, transcriptomic and biochemical data indicated that cathepsin L is the most active and expressed endopeptidase, suggesting that protein digestion predominantly occurs via cysteine peptidases in this animal. This is a common adaptive feature among predatory arachnids such as the scorpion *T. serrulatus*<sup>13</sup> and mite hematophagous species<sup>28</sup>. mRNA coding serine peptidases and metallopeptidases were also identified in the transcriptomic analysis (Table 2); however, the enzyme activity was undetectable. As previously reported<sup>13,14,16</sup> the levels of these classes of endopeptidases are also less significant to protein digestion in scorpions, mites, and ticks. On the other hand, spiders present high levels of mRNA coding metallopeptidase and a variety of genes coding distinct isoforms of astacins. Metallopeptidase activity measure could be associated with envenomation and web recycling<sup>15</sup>. As we have demonstrated for carbohydrate digestion in *M. squalidus*, the hypothesis that nutrients ingested by harvestmen are already, at least partially, in decomposition is also corroborated by the analysis of peptidases with high activity of enzymes hydrolysing preferentially short oligomers substrates such as

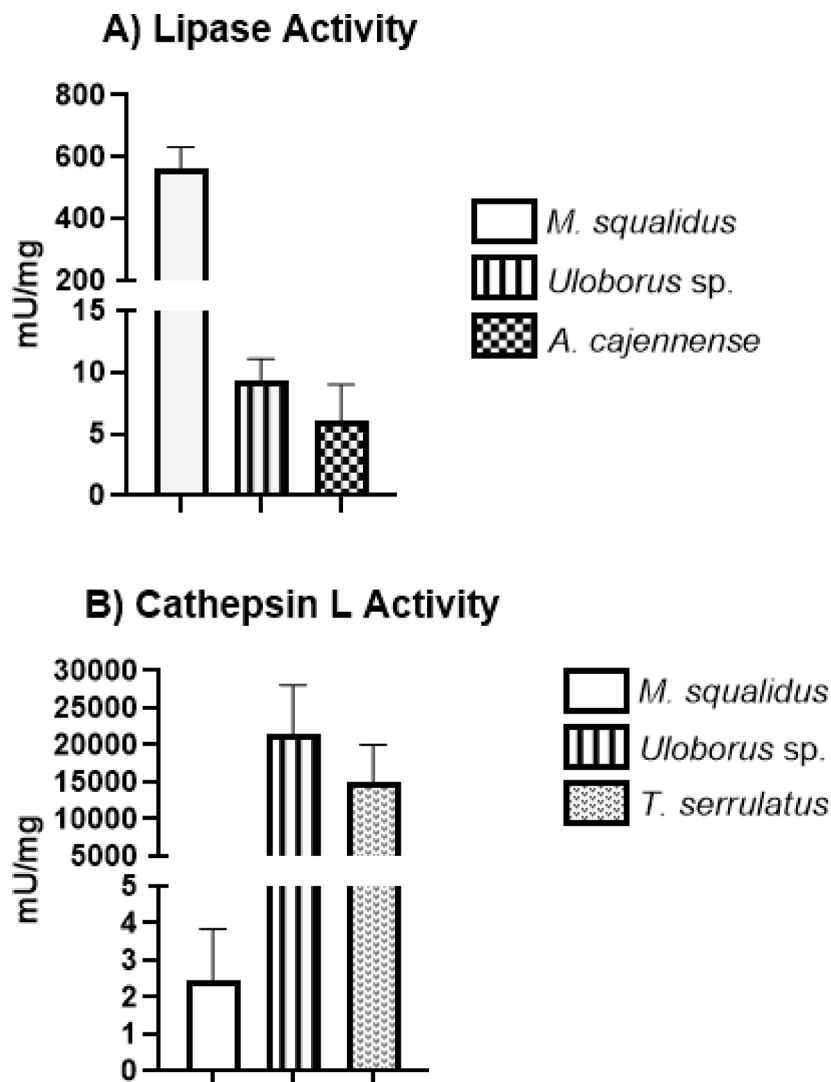


**Fig. 5.** Specific activity comparison between lipase and cathepsin L activities of *M. squalidus* and other Arachnida. The specific activities of lipase (5 A) for *M. squalidus* (561 ± 71 mU/mg), *Uloborus sp.*<sup>15</sup> (9.3 ± 1.8 mU/mg), and *Amblyomma cajennense*<sup>57</sup> (6 ± 3 mU/mg) and specific activities of cysteine peptidase (5B) (cathepsin L) for *M. squalidus* (2.44 ± 1.4 mU/mg), *Uloborus sp.*<sup>15</sup> (21,400 ± 6,700 mU/mg), and *Tityus serrulatus*<sup>13</sup> (15,000 ± 5,000 mU/mg).

carboxypeptidases and aminopeptidases and also the of abundance and diversity of mRNA coding exopeptidases (Table 3).

Finally, efficiency in lipid metabolism is the *M. squalidus* most remarkable characteristic, as revealed by enzymatic analyses. In agreement, the lipase-related transcripts were abundant in the RNA-seq analysis (Table 4), with pancreatic triacylglycerol lipase-like being the most expressed lipase gene. The predominance of lipases is a striking distinction, making the enzymatic profile of this arachnid unique and suggesting a greater reliance on lipids as an energy source or structural component in its diet. Although not among the most abundant transcripts in the transcriptome, high catalytic efficiency and/or the cumulative activity of several isoforms could explain the elevated value of lipase enzymatic activity observed. Mammalian lipases have two distinct structural forms: the closed one, where the lid covers the active site, and the open one where a colipase binds to lipase  $\beta$  barrel and also to the lid in the presence of substrate. Insects' lipases do not have the lid and are permanently in their open form<sup>29</sup> which suggests an adaptation to the absence of a colipase since this protein is not present in Insects. However, Arachnida lipases alignment sequences, other than Opiliones, suggest the presence of a lid covering the active site (Supplementary Fig. 1). However, modelling results suggested that the alpha-helix structure of the mammalian lid was replaced by a shorter loop at *M. squalidus* digestive lipase and a long alpha-helix at spider lipases. This might be related to the differences observed in lipase velocities among *M. squalidus* and other Arachnida lipases and suggests possible differences of substrate specificities of these enzymes. Apparently, till now the sequence data banks do not suggest a colipase-like protein for this group. Thus, structural studies of Arachnida lipases are paramount in understanding their mechanism of regulation, specificity and catalysis.

### Opiliones and its digestive enzymes in arachnid phylogeny

The phylogenetic position of the Opiliones within the arachnids and even Arachnida as a monophyletic group remains a subject of debate<sup>30</sup>. A study that combined cladistic and molecular analyses, focusing on the 18 S rRNA gene and the D3 region of the 28 S rRNA gene, suggests that Opiliones belong to the Dromopoda clade, along with other arachnids such as scorpions and solifugae<sup>31</sup>. A more recent study utilizing a substantial dataset comprising up to 3,644 loci has proposed an alternative clade comprising Opiliones, Ricinulei, and Solifugae<sup>32</sup>. However, knowledge regarding the digestive physiology and transcriptomics of species from these groups is still unexplored. The increase in molecular data of this group can help in new phylogeny studies to support new phylogenies. Our data Xiphosura, Scorpiones, and Araneae sequence identities among Euchelicerata already based on Blastp results of *M. squalidus* midgut transcriptome reveal a prevalence of sequenced and available at public databank (Supplementary Fig. 2). The most frequent species matches found in the unigenes' best hits of *M. squalidus* midgut are with the Xiphosura species, *Limulus polyphemus* (2,945), underscoring the molecular similarities between *M. squalidus* and basal arachnids/Chelicerata, essentially in-housekeeping genes, but also for critical digestive enzymes (e.g. alpha-L-fucosidase-like isoform x1 - TPM 1120.54). The following main matches are with two Scorpiones, *Centruroides vittatus* (2,005) and *Centruroides sculpturatus* (1,390). These occurrences agree with the phylogeny proposed by Giribet et al., 2001. The increase in data on digestive enzymes and/or other tissue transcriptome might help in future phylogenetic analysis of Opiliones.

### Genes involved in inhibitory, defense mechanisms, and toxin-like functionalities present at opiliones midgut

Midgut transcriptomic analyses of non-venomous spiders and other non-venomous Arachnida species have shown that some genes usually translated as proteins found at the venom gland, such as some metallopeptidases<sup>13–15</sup>, peptidase inhibitors<sup>33</sup>, phospholipase A2<sup>13,14</sup>, and toxins<sup>15</sup> are present at the digestive system and mainly at the midgut. These data had also been confirmed by proteomic midgut analysis of different Arachnida species suggesting a common ancestor between digestive and venom enzymes with a specialization of the last ones to gain distinct catalytic function and specificities<sup>14,34</sup>.

This is also true for Opiliones. Transcripts encoding toxin-like proteins, such as U-24 ctenitoxin, scoloptoxin, dermo necrotic toxin, and phospholipase A2 were detected. Although *M. squalidus* lacks venom glands, these proteins may have non-venomous roles, such as predigestion or defense, for this harvestmen species. Furthermore, the significant presence of glutathione S-transferases (GSTs), with multiple isoforms highly expressed, highlights their potential involvement in detoxification pathways and protection against oxidative stress<sup>35</sup> possibly to neutralize ingested toxins or other products of its saprophytic digestion.

Four-domain peptidase inhibitors (FDPI) and leukocyte elastase inhibitors (LEI) were the most expressed peptidase inhibitors in *M. squalidus* and showed significant transcription levels (Supplementary Table 3). These inhibitors likely play critical roles in protecting midgut tissues from enzymatic damage caused by peptidases, thus maintaining the structural integrity of the digestive system. However, some common serine peptidase inhibitors identified in spiders are not identified in *M. squalidus* suggesting distinct adaptations to prey peptidases ingested during feeding.

Additionally, the identification of peritrophin-like proteins suggests the formation of a peritrophic membrane. Peritrophic membranes in insects usually provide a barrier against pathogens and digestion compartmentalisation<sup>36,37</sup>. However, to harvestmen, indigestible particles and cellular excretes are first enveloped by peritrophic membranes in the anterior part of the midgut and then pass into the posterior section where they are wrapped in a peritrophic envelope consisting of many peritrophic membranes and pressed together to form a sizeable faecal pellet<sup>11</sup>. This compartmentalization of the faecal pellet by the peritrophic membrane is similar to that already described in ticks. Mites and ticks present a peritrophic membrane as an uneven single layer with a variable thickness between larvae, nymphs, and adult females, covering the whole surface of the midgut epithelium. After food repletion, the peritrophic membrane becomes thicker and thicker, winding and multi-layered.

The NPC intracellular cholesterol transporter genes, also highly expressed, point to active lipid metabolism, specifically in cholesterol regulation, transport, and efflux of cholesterol. This suggests that *M. squalidus* may rely on efficient cholesterol transport mechanisms to support its metabolic processes, possibly reflecting adaptations to specific dietary and ecological requirements, such as the transport of lipids.

As previously mentioned, harvestmen produce and secrete volatile compounds, mainly quinone derivatives. The characterisation of their intermediate products suggests acetate, propionate, and malonyl-CoA as synthesis precursors derived from fat acids and use the fatty acid synthesis pathway associated with polyketide synthase. The association of the dependence of fat acid-derived products to odour synthesis at the scent glands and our data that *M. squalidus* present high lipase activities suggests the connection between digestion and the scent gland products.

The corroboration of this hypothesis would be possible by analysing the expressed genes and protein production at the scent gland of harvestmen species to identify the molecules involved in each step of odoriferous molecule synthesis.

## Methodology

### Sample collection and maintenance

Specimens of *M. squalidus* used in this project (SISBIO authorization for sampling 87645-1 / CEUA ethics declaration 4715300123) were collected during two field expeditions, the first in March 2023 and the second in January 2024, at the Rio dos Pilões Private Natural Heritage Reserve (RPPN), located in the municipality of Santa Isabel, São Paulo, Brazil. Species identification was confirmed by Dr. Ricardo Pinto-da-Rocha, from the Instituto de Biociências, Universidade de São Paulo.

The collected adult female and male harvestmen were transported to the Laboratory of Biochemistry at the Instituto Butantan, where they were dissected to obtain sections of the midgut (MG), scent glands (SG), and carcass. Tissue dissection was performed under a stereomicroscope, using scissors and tweezers, and after immobilization of the specimens on ice for approximately 5 min. To dissect the tissues, the carapace was peeled back from the posterior to the anterior margin. The SGs were located internally, attached to the ozopores (Supplementary Fig. 3-A), while the MG was accessed through the ventral part of the animal's carcass (Supplementary Fig. 3-B). The dissected sections were separately stored in microtubes and kept at -80 °C until further use for homogenate preparation or genetic material extraction. Specimens not immediately dissected were housed in acrylic boxes with water and fed *ad libitum* on a diet of crickets.

### Enzymatic activity analyses

#### Sample preparation and assay conditions

The MG of a single adult harvestman (male or female) was prepared in 500 µL of ultrapure water for the enzymatic activity assays. MG tissues were macerated using a Potter-Elvehjem homogenizer and centrifuged at 16,000 x g for 30 min. The soluble fraction obtained from this step was used for total protein quantification and enzymatic assays. In total, 8 distinct homogenate samples were analysed. This study has measured 11 distinct enzymes, categorised into three primary classes: carbohydrases ( $\alpha$ -amylase, hexosaminidase,  $\alpha$ -L-fucosidase,  $\alpha$ -mannosidase, and chitinase), peptidases (serine peptidase, cysteine peptidase, aminopeptidase, carboxypeptidase, and metallopeptidase) and, lipases (Supplementary Fig. 4).

The total protein content in the homogenates was estimated using the BCA method (bicinchoninic acid) with absorbance readings at 562 nm<sup>38</sup>. This value was determined by comparing the slopes of standard curves prepared with diluted egg albumin (10x) and MG homogenates.

Enzymatic reactions were conducted using specific substrates and assay conditions (Table 6). All enzymatic assays were performed at 30 °C under pH and molarity conditions previously tested for the spider *Uloborus* sp<sup>15</sup>. The Cathepsin L enzyme assay involved a 30 min pre-incubation period at 30° in pH 3.5 of the homogenate to activate the zymogen before the addition of the substrate.

Enzyme assays employed substrates with chromogenic or fluorescent properties, whose concentrations were measured over time. Standard curves for each detectable product were generated. MG homogenates from eight individuals (five males and three females) were individually analyzed for total protein quantity estimation and enzymes activity detection. Specific activities were expressed as means  $\pm$  standard error of the mean.

#### Calculation of enzymatic activities (U)

- Data collected over time for each sample and enzyme assay were plotted, and a line of best fit was determined. The slope of this line represented the rate of product formation and was divided by the slope of the standard curve to calculate enzymatic activity (U) in nmol/min.

$$U(\text{nmol}/\text{min}) = \text{slope of standard curve} / \text{slope of assay}$$

- The obtained value was corrected for dilution by multiplying it by the dilution factor (2x, 5x, 10x, or 20x).

$$U_{\text{corrected}} = U \times \text{dilution factor}$$

- Absolute activity (mU) was calculated by extrapolating  $U_{\text{corrected}}$  to 1 mL of enzyme used per assay:

$$U_{\text{absolute}} = U_{\text{corrected}} \times \text{enzyme volume } (\mu\text{l}) / 1000$$

Enzymatic Assays Conditions					
Enzyme	Buffer	Substrate	Detection	Standard Curve Product	Reference
Chitinase	Citrate-phosphate 0.1 M—pH 5.25	MU-N-triacetyl-beta-D-N-N-N-triacetylchitotriose (1.7 μM)	Exc360nm/Ems460nm	4-Methylumbelliferone	Baker and Woo <sup>50</sup>
Hexosaminidase	Citrate-phosphate 0.1 M—pH 5.25	MU-N-acetyl-beta-D-glucosamine (10 μM)	Exc360nm/Ems460nm	4-Methylumbelliferone	Baker and Woo <sup>50</sup>
α-Mannosidase	Citrate-phosphate 0.1 M—pH 4.0	MU α-D-mannopyranoside (2 μM)	Exc360nm/Ems460nm	4-Methylumbelliferone	Baker and Woo <sup>50</sup>
α-L-Fucosidase	Citrate-phosphate 0.1 M—pH 5.25	MU α-L-fucopyranoside (10 μM)	Exc360nm/Ems460nm	4-Methylumbelliferone	Baker and Woo <sup>50</sup>
α-Amylase	Citrate-phosphate 0.1 M—pH 5.5	Potato starch (62 mM)	Abs550nm	Glucose	
Cysteine Peptidase (Cathepsin L)	Citrate-phosphate 0.1 M—pH 5.5	Z-Phe-Arg—MCA (10 μM)	Exc330nm/Ems430nm	7-Methylcoumarin	Alves et al. <sup>51</sup>
Metallopeptidase (Astacin)	Tris—HCl 0.5 M—pH 8.5	Casein-FiTC (0.2%)	Exc365nm/Ems525nm	*	Twining <sup>53</sup>
Carboxypeptidase	Tris—HCl 0.25 M—pH 8.0	Z-Gly-Phe (20 mM)	Abs-420 nm	Phenylalanine	Nicholson and Kim <sup>54</sup>
Aminopeptidase	Tris—HCl 0.1 M—pH 7.0	L-Leucine-p-nitroanilide (1 mM)	Abs410nm	p-Nitroaniline	Erlanger et al. <sup>55</sup>
Lipase	Tris—HCl 0.1 M—pH 8.5	Dimercapto-1-Propanol Tributryrate (0.22 mM)	Abs405nm	Cysteine	Choi et al. <sup>56</sup>
Serine Peptidase (Trypsin)	Tris—HCl 0.1 M—pH 7.0	Z-Phe-Arg—MCA (10 μM)	Exc330nm/Ems430nm	7-Methylcoumarin	Alves et al. <sup>51</sup>

**Table 6.** Conditions for enzymatic assays, including buffer solutions, substrate concentrations, detection methods, and products. Corresponding products, chromogenic or fluorescent, were respectively measured in spectramax 190 (absorbance) or GeminiXPS (fluorescence - corresponding excitation (Exc)/emission (Ems) wavelengths).

- Specific activity (mU/mg) was obtained by dividing the absolute activity by the total protein concentration in the homogenate:

$$U_{specific} = U_{absolute} / total\ protein$$

### Midgut transcriptomic analysis

Total RNA was individually extracted from the midgut (MG) of three adult females of *M. squalidus*. Tissue samples were preserved at  $-80^{\circ}\text{C}$  until processing. Three RNA extractions were performed using the TRIzol Reagent (Invitrogen) according to the manufacturer's protocol. Briefly, tissues were homogenized in 500 μL of TRIzol using a plastic pestle. After homogenization, RNA was isolated following the reagent's standard protocol and resuspended in 20 μL of DEPC water. The quality of the three extracted RNA was evaluated using a Nanodrop spectrophotometer (Thermo Fisher Scientific) to assess purity, and quantitative analyses were performed by Qubit, with an RNA HS Assay kit. RNA-seq libraries were prepared using the Illumina TruSeq Stranded RNA Core Kit according to manufacturer's instructions and  $2 \times 100$  bp reads sequenced on an Illumina NextSeq 2000 platform.

The raw reads quality was assessed using FastQC (<https://www.bioinformatics.babraham.ac.uk/projects/fastqc/>). Low-quality bases (Phred score < 30) and adapter sequences were removed using Trimmomatic<sup>39</sup> with the parameters CROP:98, HEADCROP:13, TRAILING:30, LEADING:30, SLIDINGWINDOW:5:30, and ILLUMINACLIP. Ribosomal RNA contaminants were removed using BBDuk (BBTools package) using reference sequences from the ribokmers.fa.gz file.

A *de novo* assembly was performed using Trinity v2.15.1<sup>40</sup> with default parameters. Protein-coding sequences were predicted using TransDecoder.LongOrfs and TransDecoder.Predict (<http://transdecoder.sf.net>), validated with HMMER3<sup>41</sup> against PFAM database<sup>42</sup> for domain recognition. Only the longest isoforms obtained with the Trinity script get\_longest\_isoform\_seq\_per\_trinity\_gene.pl were retained in the final transcript set from the protein predicted transcript set. The completeness of the transcriptome assembly was evaluated with BUSCO v5<sup>43</sup> using the Arthropoda and Eukaryota single-copy ortholog databases.

Functional annotation of the assembled transcripts was performed using OmicsBox v3.3.2 (BioBam)<sup>44</sup>. Transcripts were compared to the RefSeq invertebrate protein database (<ftp.ncbi.nlm.nih.gov/refseq/release/invertebrate/> - September/2024) using BLASTp with an e-value threshold of  $1\text{E}-3$ . Gene Ontology (GO) terms were assigned to transcripts, and protein domains were identified using InterProScan<sup>45</sup>. The online tool WEGO (Web Gene Ontology Annotation Plot)<sup>46</sup> was used to generate the summarized GO annotation plot from the data exported from OmicsBox. All annotation results, in table format, were integrated and analyzed using Blast2GO. Pie charts were assembled with GraphPad Prism software version 8.2.1.

Gene expression levels were quantified using RSEM<sup>47</sup> with alignment performed using Bowtie2<sup>48</sup>. Expression values were normalized and reported as TPM (Transcripts Per Million) and the mean between the three samples was calculated and used as the TPM value. The depth of the libraries was measured using the transcript.bam data generated by RSEM, using the samtools<sup>49</sup>. To analyse the digestive enzyme annotations, only those unigenes with a TPM value greater than 50 were used.

## Data availability

The raw RNA-seq sequence data from the three \*M. squalidus\* midgut samples will be available in the Short Read Archive (SRA) GenBank database <https://www.ncbi.nlm.nih.gov/genbank>: BioProject (PRJNA1197991), BioSample (SAMN45817013).

Received: 19 March 2025; Accepted: 29 August 2025

Published online: 24 September 2025

## References

- Kury, A. B., Mendes, A. C., Cardoso, L., Kury, M. S. & Granado, A. D. A. WCO-Lite: online world catalogue of harvestmen (Arachnida, Opiliones): Version 1.0—checklist of all valid nomina in Opiliones with authors and dates of publication up to 2018. (2020).
- Cohen, A. C. Extra-oral digestion in predaceous terrestrial arthropoda. *Ann. Rev. Entomol.* **40** (1), 85–103 (1995).
- Eisner, T., Rossini, C., González, A. & Eisner, M. Chemical defence of an opilionid (*Acanthopachylus aculeatus*). *J. Exp. Biol.* **207** (8), 1313–1321 (2004).
- Höfer, E. Über Das Sekret der sogenannten Stinkdrüsen der opilionen. *Archiv Für Die Gesamte Physiologie Des. Menschen Und Der Tiere.* **118** (9), 599–630 (1907).
- Rasputnig, G., Fauler, G., Leis, M. & Leis, H. J. Chemical profiles of scent gland secretions in the cyphophthalmid opilionid harvestmen, *Siro duricorius* and *S. exilis*. *J. Chem. Ecol.* **31**, 1353–1368 (2005).
- Rasputnig, G., Schaidler, M., Stabentheiner, E., Leis, H. J. & Karaman, I. On the enigmatic scent glands of dyspnoan harvestmen (Arachnida, Opiliones): first evidence for the production of volatile secretions. *Chemoecology* **24**, 43–55 (2014).
- Vieira, M. L. S. et al. Chemical and evolutionary analysis of the scent gland secretions of two species of gonyleptes kirby, 1819 (Arachnida: opiliones: Laniatores). *Chemoecology* **33** (1), 1–15 (2023).
- Rasputnig, G. et al. Chemosystematics in the opiliones (Arachnida): a comment on the evolutionary history of alkylphenols and benzoquinones in the scent gland secretions of L. aniatores. *Cladistics* **31** (2), 202–209 (2015).
- Rocha, D. F., Wouters, F. C., Machado, G. & Marsaioli, A. J. First biosynthetic pathway of 1-hepten-3-one in *Iporangaia pustulosa* (Opiliones). *Sci. Rep.* **3** (1), 3156 (2013).
- Rocha, D. F. et al. Harvestmen phenols and benzoquinones: characterisation and biosynthetic pathway. *Molecules* **18** (9), 11429–11451 (2013).
- Pinto-da-Rocha, R., Machado, G. & Giribet, G. (eds) *Harvestmen: the Biology of Opiliones* (Harvard University Press, 2007).
- Becker, A. & Peters, W. The ultrastructure of the midgut and the formation of peritrophic membranes in a harvestmen, phalangium *Opilio* (Chelicerata Phalangida). *Zoomorphology* **105** (5), 326–332 (1985).
- Fuzita, F. J. et al. Biochemical, transcriptomic and proteomic analyses of digestion in the Scorpion *tityus serrulatus*: insights into function and evolution of digestion in an ancient arthropod. *PLoS One*, **10**(4), e0123841. (2015).
- Fuzita, F. J., Pinkse, M. W., Patane, J. S., Verhaert, P. D. & Lopes, A. R. High throughput techniques to reveal the molecular physiology and evolution of digestion in spiders. *BMC Genom.* **17**, 1–19 (2016).
- Valladão, R., Neto, O. B. S., de Oliveira Gonzaga, M., Pimenta, D. C. & Lopes, A. R. Digestive enzymes and Sphingomyelinase D in spiders without venom (Uloboridae). *Sci. Rep.* **13** (1), 2661 (2023).
- Moreti, R., Perrella, N. N. & Lopes, A. R. Carbohydrate digestion in ticks and a digestive  $\alpha$ -l-fucosidase. *J. Insect. Physiol.* **59** (10), 1069–1075 (2013).
- Erban, T. & Hubert, J. Digestive physiology of synanthropic mites (Acari: Acaridida). *SOAJ Entomol. Stud.* **1**, 1–37 (2012).
- Gueratto, C., Benedetti, A. & Pinto-da-Rocha, R. Phylogenetic relationships of the genus *Mischnonyx* bertkau, 1880, with taxonomic changes and three new species description (Opiliones: Gonyleptidae). *PeerJ*, **9**, e11682. (2021).
- Pereira, W., Elpino-Campos, A., Del-Claro, K. & Machado, G. Behavioral repertoire of the Neotropical harvestman *Ilhaia cuspidata* (Opiliones, Gonyleptidae). *J. Arachnology.* **32** (1), 22–30 (2004).
- Dias, B. C. & Willemart, R. H. The effectiveness of post-contact defences in a prey with no pre-contact detection. *Zoology* **116** (3), 168–174 (2013).
- Dias, B. C., da Silva Souza, E., Hara, M. R. & Willemart, R. H. Intense leg tapping behavior by the harvestmen *Mischnonyx cuspidatus* (Gonyleptidae): an undescribed defensive behavior in opiliones?? *J. Arachnology.* **42** (1), 123–125 (2014).
- Willemart, R. H. & Pellegatti-Franco, F. The spider *Enoploctenus cyclothorax* (Araneae, Ctenidae) avoids preying on the harvestmen *Mischnonyx cuspidatus* (Opiliones, Gonyleptidae). *J. Arachnology.* **34** (3), 649–652 (2006).
- Dias, J. M. O uso do olfato nos opiliões *Neosadocus maximus* e *Mischnonyx cuspidatus* (Arachnida: Opiliones: Laniatores) (Doctoral dissertation, Universidade de São Paulo). (2017).
- Mestre, L. A. M. & Pinto-da-Rocha, R. Population dynamics of an isolated population of the harvestmen *Ilhaia cuspidata* (Opiliones, Gonyleptidae), in araucaria forest (Curitiba, Paraná, Brazil). *J. Arachnology.* **32** (2), 208–220 (2004).
- Roussel, A. et al. Crystal structure of human gastric lipase and model of lysosomal acid lipase, two lipolytic enzymes of medical interest. *J. Biol. Chem.* **274** (24), 16995–17002 (1999).
- Guimarães, D. O. et al. Transcriptomic and biochemical analysis from the venom gland of the Neotropical ant *odontomachus* chelifer. *Toxicon* **223**, 107006 (2023).
- Pfeffer, S. R. NPC intracellular cholesterol transporter 1 (NPC1)-mediated cholesterol export from lysosomes. *J. Biol. Chem.* **294** (5), 1706–1709 (2019).
- Clara, R. O. et al. Boophilus *Microplus* cathepsin L-like (BmCL1) cysteine protease: specificity study using a peptide phage display library. *Vet. Parasitol.* **181** (2–4), 291–300 (2011).
- Han, W. K., Zhang, H. H., Tang, F. X. & Liu, Z. W. Characterization of lipases revealed tissue-specific triacylglycerol hydrolytic activity in spodoptera *Frugiperda*. *Insect Science* (2024).
- Ballesteros, J. A. et al. Comprehensive species sampling and sophisticated algorithmic approaches refute the monophyly of arachnida. *Mol. Biol. Evol.* **39** (2), msac021 (2022).
- Giribet, G., Edgecombe, G. D., Wheeler, W. C. & Babbitt, C. Phylogeny and systematic position of opiliones: A combined analysis of chelicerate relationships using morphological and molecular data 1. *Cladistics* **18** (1), 5–70 (2002).
- Sharma, P. P. et al. Phylogenomic interrogation of arachnida reveals systemic conflicts in phylogenetic signal. *Mol. Biol. Evol.* **31** (11), 2963–2984 (2014).
- Neto, O. B. S. et al. Spiders' digestive system as a source of trypsin inhibitors: functional activity of a member of atracotoxin structural family. *Sci. Rep.* **13** (1), 2389 (2023).
- Walter, A. et al. Characterisation of protein families in spider digestive fluids and their role in extra-oral digestion. *BMC Genom.* **18**, 1–13 (2017).
- Ranson, H. & Hemingway, J. Mosquito glutathione transferases. *Methods Enzymol.* **401**, 226–241 (2005).
- Dias, R. O. et al. Domain structure and expression along the midgut and carcass of peritrophins and cuticle proteins analogous to peritrophins in insects with and without peritrophic membrane. *J. Insect. Physiol.* **114**, 1–9 (2019).
- Terra, W. R., Ferreira, C. & Silva, C. P. *Molecular Physiology and Evolution of Insect Digestive Systems* (Springer International Publishing AG, 2023).

38. Smith, P. E. et al. Measurement of protein using bicinchoninic acid. *Anal. Biochem.* **150** (1), 76–85 (1985).
39. Bolger, A. M., Lohse, M. & Usadel, B. Trimmomatic: a flexible trimmer for illumina sequence data. *Bioinformatics* **30** (15), 2114–2120 (2014).
40. Grabherr, M. G. et al. Trinity: reconstructing a full-length transcriptome without a genome from RNA-Seq data. *Nat. Biotechnol.* **29** (7), 644 (2011).
41. Eddy, S. R. Accelerated profile HMM searches. *PLoS Comput. Biol.* **7** (10), e1002195 (2011).
42. Finn, R. D. et al. Pfam: the protein families database. *Nucleic Acids Res.* **42** (D1), D222–D230 (2014).
43. Simão, F. A., Waterhouse, R. M., Ioannidis, P., Kriventseva, E. V. & Zdobnov, E. M. BUSCO: assessing genome assembly and annotation completeness with single-copy orthologs. *Bioinformatics* **31** (19), 3210–3212 (2015).
44. Götz, S. et al. High-throughput functional annotation and data mining with the Blast2GO suite. *Nucleic Acids Res.* **36** (10), 3420–3435 (2008).
45. Hunter, S. et al. InterPro: the integrative protein signature database. *Nucleic Acids Res.* **37** (suppl\_1), D211–D215 (2009).
46. Ye, J. et al. WEGO 2.0: a web tool for analysing and plotting GO annotations, 2018 update. *Nucleic Acids Res.* **46** (W1), W71–W75 (2018).
47. Li, B. & Dewey, C. N. RSEM: accurate transcript quantification from RNA-Seq data with or without a reference genome. *BMC Bioinform.* **12**, 1–16 (2011).
48. Langmead, B. & Salzberg, S. L. Fast gapped-read alignment with bowtie 2. *Nat. Methods.* **9** (4), 357–359 (2012).
49. Li, H. et al. The sequence alignment/map format and samtools. *Bioinformatics* **25** (16), 2078–2079 (2009).
50. Baker, J. E. & Woo, S. M.  $\beta$ -glucosidases in the rice weevil, *sitophilus oryzae*: purification, properties, and activity levels in wheat- and legume-feeding strains. *Insect Biochem. Mol. Biol.* **22**, 495–504 (1992).
51. Alves, L. C., Almeida, P. C., Franzoni, L., Juliano, L. & Juliano, M. A. Synthesis of N alpha-protected aminoacyl 7-amino-4-methylcoumarin amide by phosphorous oxychloride and Preparation of specific fluorogenic substrates for Papain. *Pept. Res.* **9**, 92–96 (1996).
52. Noeltling, G. & Bernfeld, P. Sur les enzymes amylolytiques III. La  $\beta$ -amylase: dosage d'activité et contrôle de l'absence d' $\alpha$ -amylase. *Helv. Chim. Acta.* **31**, 286–290 (1948).
53. Twining, S. S. Fluorescein isothiocyanate-labeled casein assay for proteolytic enzymes. *Anal. Biochem.* **143**, 30–34 (1984).
54. Nicholson, J. A. & Kim, Y. S. A one-step l-amino acid oxidase assay for intestinal peptide hydrolase activity. *Anal. Biochem.* **63**, 110–117 (1975).
55. Erlanger, B. F., Kokowsky, N. & Cohen, W. The Preparation and properties of two new chromogenic substrates of trypsin. *Arch. Biochem. Biophys.* **95**, 271–278 (1961).
56. Choi, S. J., Hwang, J. M. & Kim, S. I. A colorimetric microplate assay method for high throughput analysis of lipase activity. *BMB Rep.* **36**, 417–420 (2003).
57. Filietáz, C. F. T. Caracterização da digestão de lípidos em vetores hematófagos e o papel fisiológico das lipases (Doctoral thesis, Universidade de São Paulo). (2011).

## Acknowledgements

The authors sincerely acknowledge Ighor Fernandes and Ryan Romão for the specimen collecting support; Erica Fiadi and Jaderlina Todão for the material preparation and sequencing support; and Chris Cardoso and the Bioinformatics DOJO group for the bioinformatics expertise shared. This work used resources from two High-Performance Computing Systems: one from the Center for Bioinformatics and Computational Biology (NBBC) at Butantan Institute, and the other from the Genetics and Biodiversity Laboratory (LGBIO) at Goiás Federal University, which was supported by the National Institutes for Science and Technology (INCT) in Ecology, Evolution and Biodiversity Conservation, supported by MCTIC/CNPq (proc. 465610/2014-5) and FAPEG (proc. 201810267000023). The research was supported by the Brazilian research agencies FAPESP (Grant number 2017/08103-4) and CAPES.

## Author contributions

J.O.S. Specimens collection; experimental execution, bioinformatics, data analysis and manuscript composition; V.L.V. Critical reading, experimental design and execution; R.O.D. Critical reading and bioinformatics analysis; C.F. Critical reading; W.R.T. Critical reading; R.P.R. Critical reading and species identification; A.R.L. Experimental design, data analysis and manuscript composition.

## Declarations

### Competing interests

The authors declare no competing interests.

## Additional information

**Supplementary Information** The online version contains supplementary material available at <https://doi.org/10.1038/s41598-025-18180-x>.

**Correspondence** and requests for materials should be addressed to A.R.L.

**Reprints and permissions information** is available at [www.nature.com/reprints](http://www.nature.com/reprints).

**Publisher's note** Springer Nature remains neutral with regard to jurisdictional claims in published maps and institutional affiliations.

**Open Access** This article is licensed under a Creative Commons Attribution-NonCommercial-NoDerivatives 4.0 International License, which permits any non-commercial use, sharing, distribution and reproduction in any medium or format, as long as you give appropriate credit to the original author(s) and the source, provide a link to the Creative Commons licence, and indicate if you modified the licensed material. You do not have permission under this licence to share adapted material derived from this article or parts of it. The images or other third party material in this article are included in the article's Creative Commons licence, unless indicated otherwise in a credit line to the material. If material is not included in the article's Creative Commons licence and your intended use is not permitted by statutory regulation or exceeds the permitted use, you will need to obtain permission directly from the copyright holder. To view a copy of this licence, visit <http://creativecommons.org/licenses/by-nc-nd/4.0/>.

© The Author(s) 2025